HHS Public Access

Author manuscript

Sci Transl Med. Author manuscript; available in PMC 2019 June 27.

Published in final edited form as:

Sci Transl Med. 2018 June 27; 10(447): . doi:10.1126/scitranslmed.aap9328.

Preclinical assessment of antiviral combination therapy in a genetically humanized mouse model for hepatitis delta virus infection

Benjamin Y. Winer[1], **Elham Shirvani-Dastgerdi**[#1], **Yaron Bram**[#2], **Julie Sellau**[1], **Benjamin E. Low**[3], **Heath Johnson**[1], **Tiffany Huang**[1], **Gabriela Hrebikova**[1], **Brigitte Heller**[1], **Yael Sharon**[1], **Katja Giersch**[4], **Sherif Gerges**[1], **Kathleen Seneca**[5], **Mihai-Alexandru Pais**[1], **Angela S. Frankel**[2], **Luis Chiriboga**[6], **John Cullen**[7], **Ronald G. Nahass**[5], **Marc Lutgehetmann**[8], **Jared Toettcher**[1], **Michael V. Wiles**[3], **Robert E. Schwartz**[2], and **Alexander Ploss**[1,**]

[1]Department of Molecular Biology, Princeton University, Lewis Thomas Laboratory, Washington Road, Princeton, New Jersey, NJ 08544, USA

[2]Division of Gastroenterology & Hepatology, Department of Medicine, Weill Medical College of Cornell University, New York, NY 10021, USA

[3]Department of Technology Evaluation and Development, The Jackson Laboratory 600 Main Street, Bar Harbor, Maine, 04609-1500 USA

[4]I. Department of Internal Medicine, Center for Internal Medicine, University Medical Center Hamburg-Eppendorf, Hamburg, Germany

[5]ID Care, 105 Raider Boulevard, Hillsborough, NJ 08844, USA

[6]Department of Pathology, New York University Medical Center, New York, NY 10016, USA

[7]Department of Population Health and Pathobiology, North Carolina State University College of Veterinary Medicine, Raleigh, NC 27607, USA

[8]Institute of Microbiology, Virology and Hygiene, University Medical Hospital Hamburg-Eppendorf, Hamburg, Germany

[#] These authors contributed equally to this work.

Abstract

Chronic delta hepatitis, caused by hepatitis delta virus (HDV), is the most severe form of viral hepatitis, affecting at least 20 million hepatitis B virus (HBV)-infected patients worldwide. HDV/HBV co- or super- infections are major drivers for hepatocarcinogenesis. Antiviral treatments exist only for HBV and can only suppress but not cure infection. Development of more

[**]Correspondence to: Alexander Ploss, aploss@princeton.edu, phone: (609) 258-7128.

AUTHOR CONTRIBUTIONS

B.Y.W. and A.P. conceived the study, designed and performed experiments, analyzed data and wrote the manuscript. E.S.D., Y.B., J.S., B.E.L., H.J., J.T., M.V.W. and R.E.S. performed experiments and analyzed data. T.H., G.H., B.H., Y.S., S.G., M.A.P., A.S.F, and L.C. performed experiments. J.C. performed the histopathological analysis. R.G.N and K.S. provided patient serum and technical support. K.G. and M.L. provided valuable reagents.

Additional information can be found in the Supplemental Materials and Methods section.

Competing financial interests. The authors declare no relevant conflicts of interest.

effective therapies has been impeded by the scarcity of suitable small animal models. Here, we created a transgenic (tg) mouse model for HDV expressing the functional receptor for HBV and HDV, the human sodium taurocholate co-transporting peptide NTCP. Both HBV and HDV entered hepatocytes in these mice in a glycoprotein-dependent manner, but one or more post-entry blocks prevented HBV replication. In contrast, HDV caused persistent infection in hNTCP tg mice co-expressing the HBV envelope, consistent with HDV dependency on the HBV surface antigen (HBsAg) for packaging and spread. In immunocompromised mice lacking functional B, T, and NK cells, viremia lasted at least 80 days but resolved within 14 days in immunocompetent animals, demonstrating that lymphocytes are critical for controlling HDV infection. Although acute HDV infection did not cause overt liver damage in this model, cell-intrinsic and cellular innate immune responses were induced. We further demonstrated that single and dual treatment with myrcludex B and lonafarnib efficiently suppressed viremia but failed to cure HDV infection at the doses tested. This small animal model with inheritable susceptibility to HDV opens opportunities for studying viral pathogenesis, immune responses, and for testing novel HDV therapeutics.

One sentence summary:

An inbred mouse model for HDV infection can be used to study virally-induced immune responses and for testing antiviral therapeutics.

Introduction:

Chronic hepatitis delta (CHD), caused by hepatitis delta virus (HDV), was first described as a distinct form of blood-borne hepatitis in 1977 (1). HDV is a 1679-nucleotide, enveloped, negative-sense RNA satellite virus and sole member of the delta virus genus (reviewed in (2)). The small HDV circular genome is only ca 1.7 kb in length and is stabilized by extensive intramolecular base pairing. HDV encodes a single open reading frame (ORF) encoding the delta antigen (HDAg), which exists as two isoforms, the small and large HDAg (3). As HDV requires the HBV surface antigens (HBsAg) for packaging of viral particles and thus is dependent the presence of HBV, it is considered a subviral satellite. Consequently, the early steps of HDV entry into hepatocytes follow the same mechanism as HBV. Once within the hepatocyte, a nuclear localization signal on HDAg-L triggers the translocation of the HDV nucleocapsid to the nucleus where the viral genome is replicated. The small size of the HDV genome results in the virus' reliance on host enzymes, including cellular RNA polymerases, to successfully replicate (reviewed in (4)). The incoming RNA serves as the template for transcripts longer than the size of the virus' genome. Such multimeric, linear RNAs contain at least two copies of the antigenomic ribozyme, releasing unit-length linear RNA following self-cleavage. Antigenomic RNA is circularized and forms the template for new genomic RNAs following similar intermediate steps.

Co-infection with HBV/HDV or super-infection of chronic HBV patients with HDV usually progresses to delta persistence, frequently resulting in fibrosis, cirrhosis, and hepatocellular carcinoma (HCC). Although HDV and HBV infection can be prevented by prophylactic vaccination, effective and curative HDV treatments do not exist.

Studies of the mechanisms of viral persistence, pathogenesis and development of effective therapies for CHD have been hampered by the scarcity of experimentally tractable animal models. HDV has a narrow and poorly understood host tropism limited to infections in humans and a few primate species that are also susceptible to HBV (5). The only available small animal models susceptible to HBV/HDV co- or super-infections are human liver chimeric mice (6), which are highly immunocompromised animals growing a partially human liver. Woodchucks as a small animal model have also played an important role in understanding HDV viral infection and persistence *in vivo*. HDV pseudotyped with the envelope proteins from woodchuck hepatitis virus (WHV), a hepadnavirus related to HBV, can infect cultured woodchuck hepatocytes and lead to HDV persistence in woodchucks chronically infected with WHV (7–10). Although the woodchuck model has contributed significantly to our understanding of HDV persistence and genome stability, there is a dearth of available reagents to study in-depth the host immune response to persistent HDV infection in this model. An inbred mouse model – such as the one presented in our current study – holds the potential to overcome many of these caveats. The challenge is to systematically identify and overcome any restrictions to HBV and HDV growth in murine cells. Differences between the protein sequences of the sodium taurocholate co-transporting peptide NTCP (SLC10A1), the receptor for HBV and HDV (11, 12), in humans and non-permissive species, such as rodents, pigs and certain primate species, explain the block at the level of viral entry (13, 14) but not necessarily at other later stages in the viral life-cycles. Expression of human NTCP (hNTCP) is sufficient to mediate HDV uptake and infection in mouse hepatocytes *in vitro* (15), but these cells remain resistant to HBV (15, 16). These observations were corroborated in mice transgenically expressing hNTCP or a humanized allele of NTCP that supports HDV. However, susceptibility was age-dependent and required inoculation with very high doses of HDV (17, 18).

Here, we created a mouse model in which hNTCP is expressed under the control of the human regulatory elements. Immunodeficient mice co-expressing both hNTCP and 1.3× HBV transgenes support persistent HDV infection for more than 80 days. In contrast, immunocompetent hNTCP/1.3× HBV transgenic mice became acutely viremic but eventually cleared the infection within 30 days. We demonstrate that while combination treatment with myrcludex B and lonafarnib – two drug candidates for CHD – can efficiently suppress viremia, each drug alone or together failed to cure HDV infection. Our model is amenable to genetic manipulations, robust and high in throughput and thus lends itself for studying chronic hepatitis *in vivo* and systematically testing novel therapies targeting HDV.

Results

Transgenic expression of hNTCP facilitates HBV uptake into hepatocytes *in vivo*.

To further probe the HBV and HDV life cycles in an experimentally tractable animal model, we generated mice transgenically expressing a bacterial artificial chromosome (BAC) containing part of human chromosome 14, which includes the *SLC10A1* gene encoding NTCP and upstream human regulatory elements (henceforth hNTCP/BAC, fig. S1). Quantitative RT-PCR (qRT-PCR) analysis demonstrated that hNTCP is expressed in the liver

of mice but not in other tissues such as the kidney, brain, lung, large or small intestines (Fig. 1A, fig. S2a-d), thus mirroring the native tissue expression pattern of NTCP.

Mouse cells expressing hNTCP can support HDV infection but appear to be resistant to HBV infection (15, 16). The apparent block in HBV infection is presumably not due to a dominant negative restriction factor as heterokaryons of HBV-susceptible human and HBV-resistant mouse hepatoma cells remain permissive to infection (19). HDV and HBV share the same viral envelope, but it remains unclear whether HBV can productively enter mouse hepatocytes expressing human NTCP *in vivo* given their otherwise distinct natures. To directly test whether transgenic (tg) mouse hepatocytes can support HBV uptake, hNTCP/BAC tg mice on the immunodeficient non-obese diabetic (NOD) recombinase activating gene 1 knockout (Rag1−/−) interleukin 2 receptor gamma chain null (IL2Rγ^{NULL}) background (hNTCP/BAC-NRG), which thus lack functional B, T, and NK cells, were injected with 5-ethynyl-2′-deoxycytidine (EdC)-labeled cell culture-produced HBV (HBVcc-EdC) (Fig. 1B, C). EdC-labeling provides very sensitive means to visualize HBV DNA even while still contained within the entering viral nucleocapsids. Thus, quantification of viral uptake is uncoupled from the completion of post-entry steps. Of note, EdC-labeling did not compromise viral fitness as evidenced by the fact that HBV surface antigen (HBsAg) concentrations in cell culture supernatants, the frequency of HBV core antigen (HBcAg)+ cells, and the amount of pre-genomic RNA (pgRNA) (fig. S3a, b, c, respectively), were equivalent irrespective of whether EdC-labeled or non-labeled HBVcc was used to infect hNTCP-expressing HepG2 cells (3B10) (20). Quantitative image analysis of liver tissue sections harvested at 18 hours post challenge of hNTCP/BAC-NRG mice revealed that HBV entered up to 25% of hepatocytes (Fig. 1B). HBV entry was dependent on the presence of hNTCP expression, as the EdC signal remained at background in non-tg NRG control animals. Consistent with previously published *in vitro* data (15), there was no further evidence for productive HBV infection as neither experimental group showed an increase in serum levels of HBsAg (Fig. 1D), or HBV DNA and pgRNA in liver tissue (fig. S4a-b) at any time up to 14 days following infection with cell-culture produced HBV (HBVcc).

Previous studies in other hNTCP-expressing mouse lines injected with very large viral inocula showed that small frequencies of hepatocytes stained positive for hepatitis delta antigen (HDAg), but infection ceased within 10-14 days (17, 18). Since HDV assembly and spread is dependent on the presence of HBsAg, we hydrodynamically delivered (HDD) a 1.3× over length HBV genome to the livers of adult hNTCP/BAC-NRG mice. Consistent with previous reports (21), delivery of the 1.3× HBV genome led to sustained secretion of HBsAg (**figs.** S5a-d **and** S6). HDV RNA levels were 50-100-fold higher in the sera of hNTCP/BAC/1.3×HBV-NRG mice than in all control groups expressing one or none of the transgenes (Fig. 1E). Consistent with these observations, HDV genomic RNA (Fig. 1F) was approximately 10-fold higher in doubly tg than in hNTCP tg mice and about 500-fold higher than in non-tg mice. Likewise, anti-genomic RNA was only detectable in the doubly tg mice (Fig. 1G), providing further evidence for persistent infection (22). Anti-genomic RNA most likely forms in hNTCP tg mice but was too low to detect with the assays available, reinforcing the importance of the HBV envelope proteins in this model for HDV persistence.

During HDV's replicative cycle the adenosine in the amber stop codon in the antigenome of the HDAg is edited to an inosine by ADAR1 (23), causing a change to a tryptophan and expression of the long form of the HDAg (24). This transition from small to large HDAg results in a switch from replication to viral packaging and egress. To ascertain that this editing process takes place in this mouse model we sequenced HDV RNA isolated from serum and livers of hNTCP/BAC/1.3×HBV-NRG mice. Previous studies showed that a mixture of primarily non-edited and to a lesser extent edited HDV RNA is detectable in both tissue compartments (24, 25). Consistent with these clinical data we detected the expected mutation in the HDV genome from viral RNA isolated from the liver (fig. S7), indicating that both isoforms of the HDAg are present allowing for replication, virion packaging, and egress.

There are eight genotypes of HDV, which vary in their genome sequence by 30-50% (26). It is also known that mutations can arise in the HDV genome over the course of a chronic infection both in the woodchuck model and in humans (25, 27). To demonstrate that the observed HDV viremia was not limited to cell culture-derived HDV (HDVcc), we monitored infection with patient-derived HDV (HDVpat). hNTCP-BAC/1.3×HBV-NRG mice were challenged with either heparin column-purified HDVpat (1×10^8 GE/animal, n=6), HDVcc (1×10^9 GE/animal, n=5), or PBS injected and HDV viremia monitored over time. HBsAg levels, regardless of cohort, were stable over the 14 days of the experiment (Fig. 1H). Mice challenged with HDVpat or HDVcc became viremic with no significant difference between the two cohorts (Fig. 1I). After 14 days post HDV infection, mice were euthanized. A substantial amount of HDV RNA was isolated from the livers of both cohorts relative to the non-infected controls, demonstrating that both HDVpat and HDVcc challenged mice were productively infected with HDV (Fig. 1J).

HDV is taken up through an HBV glycoprotein-mediated mechanism in hNTCP-BAC tg mice

To demonstrate that HDV enters through an HBV glycoprotein-dependent process, we pre-treated hNTCP-BAC/1.3×HBV-NRG mice with a HBV preS1-derived peptide shown to effectively block HBV and HDV uptake in pre-clinical models and clinical trials (28, 29) (Fig. 2A). Indeed, HDV RNA levels were significantly decreased in both the serum ($p < 0.0437$) (Fig. 2B) and liver tissue ($p < 0.0477$) (Fig. 2C) of mice injected with the blocking peptide, but not with a mutant control peptide. Collectively, our data demonstrate that NTCP is a species tropism-determining factor for HBV and HDV uptake in mouse hepatocytes similar to a variety of primate species (13), but additional post-entry steps restrict HBV, but not HDV, infection in mice.

hNTCP-BAC NRG mice co-expressing a 1.3× HBV genome support persistent HDV infection.

We next aimed to determine whether HDV could achieve long-term persistence in our model. Thus, we infected hNTCP/BAC-NRG mice with HDV along with either a 1.3× HBV genome by HDD or injection with a recombinant adenovirus (rAdV) expressing only the large, middle, and small HBV envelope proteins (rAdV-HBVenv, Fig. 3A). HBsAg was detectable in the sera of both experimental cohorts (Fig. 3B) but was higher in the 1.3× HBV groups. In the case of the vector approach, expression was further validated through

bioluminescent imaging of a luciferase reporter co-expressed in the rAdV-HBVenv (Fig. 3C, 3D) and by HBsAg Western blot which detected all three forms: small (S, 35% total), medium (M, 18%), and large (L, 47%) both glycosylated and non-glycosylated (fig. S8). Of note this ratio of L-HBsAg to S-HBsAg provided by the AdV-HBV Env vector does not fully reflect the expression ratios that occur during native HBV infection. This could potentially explain the lower levels of HBsAg present in the hNTCP-BAC/1.3× AdV NRG mice. Regardless of how the HBV envelope proteins were delivered, serum HDV RNA copies rose 100-500 fold over background and remained largely stable for 84 days when the experiment was terminated.

To quantify the frequency of HDV-infected cells, we employed a proximity ligation for viral RNA (PLAYR) method (see methods for details) (30). Clusters of HDV genomic RNA-bearing cells were readily visible in hNTCP/BAC-NRG but not in NRG control mice infected with HDV (Fig. 3E). The somewhat low frequency (2-6%) (Fig. 3F) is likely attributable to the fact that only a fraction of murine hepatocytes express the HBV envelope. Prolonged HDV persistence was further corroborated by RT-qPCR, which showed an approximately 100 (hNTCP/BAC + AdV-HBVenv) to 1000 (hNTCP/BAC + 1.3×HBV HDD) fold higher HDV RNA copy number (Fig. 3G), and by HDAg Western blot analysis (fig. S9) of liver lysates from HDV-infected tg versus non-tg mice.

Next, we sought to determine whether HDV acquires adaptive mutations to augment replication in the murine cellular environment. We managed to derive full-length sequences from four of the eight persistently infected mice. In comparison to the inoculum, several mutations emerged throughout the genome (**figs.** S10, S11, S12a-b, **and** S13), including the HDV ribozyme (Rbz, Fig. 3H) and the HDAg (Fig. 3I). Although residues near the HDV Rbz cleavage site remained unaltered, an A/G change at position 46 within the Rbz domain near the P4 stem loop structure could possibly affect the RNA secondary structure of the HDV anti-genome. However, none of the mutations were consistently detected in all genomes, suggesting they do not contribute to a putative gain-of-function favoring HDV RNA replication in mice.

Single and combination therapy with Myrcludex B and Lonafarnib efficiently suppresses HDV viremia *in vivo* but does not cure HDV infection.

It was previously demonstrated that acylated peptides derived from the large HBsAg (now developed as Myrcludex B, MyrB) can block HBV and HDV virus entry in cell lines (31), primary hepatocytes (20) and in human liver chimeric mouse models (28). Recent clinical data showed that administration of MyrB to HBV/HDV co-infected patients resulted in significant decreases in HDV RNA loads (29, 32), consistent with the dependence of HDV on HBsAg. As an alternative approach for HDV treatment, inhibitors interfering with the prenylation of HDAg, and thereby its interaction with HBsAg and the subsequent release of infectious particles (33), have been tested *in vitro* and *in vivo*. Encouragingly, treatment of HDV patients with one such inhibitor, lonafarnib (LNF), resulted in a mean 1.54-log IU/mL decline in HDV RNA from baseline (34). Here, we aimed to test single and combination treatments with MyrB and LNF as therapeutics in our mouse model. We delivered a 1.3× HBV genome by HDD to hNTCP/BAC-NRG mice and infected them four days later with

HDV (Fig. 4A). Previously, viral load reductions in the serum effects have been observed in HDV/HBV co-infected patients treated with 200 mg LNF (34) and 2-20 mg MyrB (29, 32), and thus doses were scaled proportionally to the animals' body weights. We injected mice intraperitoneally with MyrB (67.6 μg/kg) and/or administered LNF orally (2.7 mg/kg). While HBsAg concentrations, as expected, were not affected by either or both treatments (Fig. 4B), HDV RNA levels in the serum dropped significantly (LNF $p=0.0001$, Dual $p< 0.0001$, MyrB $p< 0.0001$) within one week of treatment and remained around the limit of quantification at 14 days post treatment (Fig. 4C). At 14 days post treatment, mice from each cohort were euthanized to assess HDV RNA copy numbers in the liver. Notably, HDV RNA levels in the liver were significantly reduced by ~3 log (MyrB, $p= 0.0418$) and ~4.5 log (dual, $p= 0.0415$) as compared to the carrier control group, while the ~1.5 log drop (LNF) was not significant ($p= 0.0564$) (Fig. 4D). To determine whether HDV was actually cleared in any of the treatment arms, we stopped treatment and continued monitoring HDV viremia. Upon cessation of treatment, HDV viremia rebounded in LNF, MyrB, and dually treated mice, reaching pre-treatment viremia levels by 5 weeks (Fig. 4C). This rebound was corroborated by high HDV RNA levels in the livers of mice in each cohort as determined by RT-qPCR (Fig. 4E). Notably, HDV RNA copies remained largely unaffected in the serum and liver of mice treated with the carrier control. Collectively, these data establish proof-of-concept for the utility of our model for antiviral drug testing.

HDV infection in immunocompetent mice expressing hNTCP and a 1.3× HBV transgene

The pathology observed in hepatitis delta patients is attributable at least in part to the intrahepatic inflammatory milieu. To create a model that would possibly enable the analysis of delta immunopathology, we analyzed HDV infection in immunocompetent hNTCP/BAC mice on the C57BL/6 background also stably expressing a 1.3× HBV transgene (35) (Fig. 5A), thereby providing the HBsAg required for HDV propagation (Fig. 5B). Consistent with our data in immunocompromised mice, HDV infection was dependent on expression of both the hNTCP BAC and 1.3× HBV tgs (Fig. 5C, D). In the sera of doubly tg mice, HDV RNA copies were 10-50 higher than all control cohorts until day 14 post infection when viral loads decreased to levels comparable to those of the non-tg control group (Fig. 5C). In the liver tissue of both dually tg and hNTCP tg mice, HDV RNA remained high until day 14 post infection after which it decreased. In doubly tg mice, HDV RNA levels remained above background until day 30 post infection (Fig. 5D). These data suggest that HDV infection is controlled, albeit not cleared, by the murine immune system during the acute phase of infection. The immune system may exert pressure on HDV, yielding viral variants with escape mutations in the HDAg - HDV's only protein antigen. However, sequence comparison of HDV genomes from hNTCP/BAC-1.3×HBV mice on the NRG and C57BL/6 cohorts did not provide evidence for this (Fig. 5E, fig. S14).

HDV induces innate and adaptive immune responses in immunocompetent hNTCP-BAC/1.3× doubly transgenic mice

We next aimed to determine whether the murine immune system becomes activated during HDV infection and results in liver damage in our model. ALT levels were in the normal range in all mice regardless of genetic background (Fig. 6A). This is consistent with our histological analysis where only small changes, but no major histopathology, were observed

(Fig. 6B). In accordance with previously published data in human liver chimeric mice showing that HDV co-infection induces markedly greater innate immune responses in comparison to HBV mono-infection (36), we also observed changes in the expression of multiple ISGs, including *PKR, OAS-L, IP-10* and *Mx1* in hNTCP/1.3×HBV double as compared to 1.3×HBV single tg mice (Fig. 6C, D). These observations are also consistent with the MAVS-dependent induction of IFN observed in mice in which the HDV and HBV genomes were expressed by an adeno-associated virus vector system (37). Specifically in the hNTCP/1.3×HBV double tg group that supported viremia, we also observed early post infection increased frequencies of NK (Fig. 6E), NK T cells (Fig. 6F) and mucosal-associated invariant T (MAIT) cells (Fig. 6G). These immune cell subsets have been implicated in clearance of cells infected with hepatotropic pathogens (38), and, altogether, our data suggest the innate and cellular immune response may antagonize establishment of persistent HDV infection in fully immunocompetent mice.

Discussion

This study represents a step forward in developing a robust animal model for HDV infection and immunity. Here, we demonstrate that the entire HDV life cycle can be recapitulated in an inbred mouse model with inheritable susceptibility to HDV. Both HBV and HDV can enter hNTCP-expressing mouse hepatocytes *in vivo* following an HBsAg-dependent and thus native entry mechanism. Although a post-entry block prevents the completion of the HBV life-cycle, HDV replication, particle assembly and egress, are supported in the presence of the HBsAg. Both genomic and antigenomic viral RNA is detectable in the livers of HDV infected mice. Sequence analysis revealed that both edited and non-edited forms of the HDAg are present in the livers of persistently infected animals demonstrating that virions are assembled through the native mechanism. These RNA editing data are consistent with prior observations in HDV mono-infected hNTCP-tg mice (17, 18). In the serum we were only able to detect non-edited genomic RNA molecules, which is conceivably due to the combination of the overall lower viral titers in our mice as compared to patients, and the limitations in the sensitivity of the sequencing method. It should also be noted that the frequency at which the editing event occurs ranges and has been estimated at 15-30% in cell culture experiments (24). Thus, edited RNA represents only a subfraction of the total HDV RNA which may further impair detection in this model.

Previously developed human liver chimeric mice can also support HDV and HBV co-infections (6). However, such xenotransplantation models are low-throughput, expensive to generate and hampered by intra- and inter-experimental variability as well as donor-to-donor variability. Another recent model relies on vector-mediated over-expression of the HDV and HBV genomes, which arguably does not adequately mimic the inflammatory situation induced during infection (37). The inbred mouse model presented here holds the potential to overcome many of these caveats, as it is amenable to genetic manipulations and can be employed for preclinical assessment of the efficacy of entry inhibitors and other putative therapeutics. We demonstrate that single and combined administration of MyrB and LNF, two therapeutics with distinct mechanisms of action, results in HDV RNA suppression in both the serum and liver of these mice. Notably, our data suggest that co-administration of MyrB and LNF may have a synergistic effect, as evidenced by an approximately 1000-fold

decrease in HDV RNA in the liver. However, even the combination of MyrB and LNF does not seem adequate to completely abrogate HDV infection. The serum data for the monotherapies are largely in line with recently reported data from clinical trials (29, 32, 34) and thereby show the utility of our model for assessing the preclinical efficacy of novel therapeutics in a convenient animal model. In clinical trials LNF and MyrB were administered in fixed doses at twice 200 mg or once 2-20 mg of LNF(34) and MyrB (29, 32), respectively. Indeed, it is important to note that the doses used in our study do not perfectly match those of published clinical studies, corresponding to half the optimal monotherapy dose of LNF, and twice the dose of MyrB used in clinical trials. Thus, a direct comparison of their relative efficacy or respective contributions to the apparent observed synergy in this model may not be not possible. Irrespectively, our model now creates the possibility of assessing combination therapies to eliminate HDV in longer-term follow-up studies and to evaluate their effects on viremia not only in serum but also liver tissue.

We provide evidence that HDV induces both innate and adaptive immune responses, which collectively contribute to the control of HDV viremia *in vivo*. These results are distinct from the clinical course of HDV infections in patients in which the virus usually progresses to chronicity. Thus, the murine immune system may be effective at clearing HDV. Mild liver pathology was virally induced and presumably immune-mediated, and even this overall moderate phenotype was remarkable considering the animals are tolerized to the HBV transgene. Immune-mediated contribution to liver damage can thus be largely attributed to the HDV infection. It may remain challenging to establish a bona fide HBV/HDV co- or super-infection given the yet to be resolved blocks in the HBV life cycle. However, future efforts aimed at modeling a phenotype even more similar to that observed in patients could address whether liver disease is more exacerbated in HDV-infected hNTCP/BAC-1.3× HBV tg mice in which immunologic tolerance to HBV has been broken.

Materials and Methods:

Study design

This study was designed to characterize HDV infection in a genetically humanized transgenic mouse model that expresses the HBV/HDV receptor, human sodium taurocholate co-transporting peptide NTCP (hNTCP), and the HBV envelope proteins. In addition, we assessed immune responses and preclinical antiviral combination therapy against HDV in these mice. All human samples and animal work was approved by the Institutional Animal Care and Use Committee (IACUC) and Institutional Review Board (IRB) of Princeton University (IACUC # 1930-16, deemed non-human subjects research by IRB). For *in vitro* studies 3-6 biological replicates were performed; in *In vivo* experiments 4-8 mice were used per time point for longitudinal assays. Experiments were not performed in a blinded fashion.

Animals.

hNTCP BAC tg mice on the C57BL/6 and NRG backgrounds were generated as described in the Supplementary Methods. 1.3× HBV tg mice were kindly provided by Frank Chisari (The Scripps Research Institute), NRG and C57BL/6J mice were obtained from The Jackson Laboratory. All *in vivo* experiments were in accordance with protocols reviewed and

approved by the Institutional Care and Use Committees (IACUC) of Princeton University, respectively.

Generation of HBV and HDV stocks

To generate HBV stocks, HepG2.2.15 cells (39) were grown in media containing tetracycline until they reached a confluency of 100%. At this time, media was changed to DMEM F12 media supplemented with 10% FBS, 1% Pen/Strep. To produce HDV stocks, the plasmid psvL(D3) (a gift from John Taylor (Addgene plasmid # 29335) (40) containing three copies of the HDV genome was transfected into a HepG2 cell line that constitutively expresses the large, medium, and small HBV envelope proteins. Virus-containing supernatants were concentrated, and the virus was run over a HiTrap heparin column (GE, Fairfield, CA) to purify infectious virus particles from non-infectious sub-viral particles. After dialysis, virus was aliquoted into cryovial tubes and cryopreserved at −80°C until use.

Mouse infections

All mouse infections with HBV, HDV, or with rAdV were done by intravenous injection into the tail vein with 1×10^8 GE of HBV, 1×10^9 GE of HDV, or an MOI of 1×10^{10} for rAdV in a total volume of 200 μl per mouse. Mice were bled submandibularly at the indicated time points (0, 3, 7, 14, 21, and 30 days post infection), depending on experiment.

Statistical Analysis

All statistical analysis was performed with GraphPad Prism 6h software. Data are presented as means ± SEM. Multiple group comparisons were analyzed by one-way ANOVA with a Bonferroni's multiple comparisons test. P values of <0.05 were taken as being statistically significant.

Supplementary Material

Refer to Web version on PubMed Central for supplementary material.

Acknowledgements

HepG2.2.15 cells were kindly provided by Christoph Seeger (Fox Chase Cancer Center, FCCC, Philadelphia PA) and the 1.3× HBV transgenic mice by Frank Chisari (The Scripps Research Institute, La Jolla, CA). The pSVL(D3) and 1.3× HBV plasmids were gifts from John Taylor (FCCC) and Yosef Shaul (Weizmann Institute, Rehovot, Israel), respectively. Stephan Urban (University of Heidelberg, Germany) kindly provided the Myrcludex B compound. We thank Tom Muir and Felix Wojcik (both Princeton University) for help with the peptide synthesis. We thank Christina DeCoste and the Molecular Biology Flow Cytometry Resource Facility, Gary Laevsky and the Nikon Center of Excellence for generous assistance with imaging and the staff of the Molecular Biology and Microinjection Cores at The Jackson Laboratory for outstanding technical support. We are grateful to Jenna Gaska and members of the Ploss lab for critical discussions and edits of this manuscript.

Funding: This study is supported by grants from the National Institutes of Health (R01 AI079031, R01 AI107301, R21AI117213 to A.P.), a Research Scholar Award from the American Cancer Society (RSG-15-048-01-MPC to A.P.), a Burroughs Wellcome Fund Award for Investigators in Pathogenesis (to A.P.) and a Graduate fellowship from the Health Grand Challenge from the Global Health Fund of Princeton University (to B.Y.W.). The Princeton Molecular Biology Flow Cytometry Resource Facility is partially supported by the Cancer Institute of New Jersey Cancer Center Support Grant (P30CA072720), The NYU Experimental Pathology Immunohistochemistry Core Laboratory is supported in part by the Laura and Isaac Perlmutter Cancer Center Support Grant; NIH /NCI P30CA016087 and the National Institutes of Health S10 Grants; NIH/ORIP S10OD01058 and S10OD018338. B.Y.W. is a recipient of an F31 NIH/NRSA Ruth L. Kirschstein Predoctoral award from the NIAID and a graduate

fellowship from the New Jersey Commission on Cancer Research. J.S. and E.S.D. are both recipients of postdoctoral fellowships from the German Research Foundation. M.V.W. was funded by The Jackson Laboratory.

References and notes:

1. Rizzetto M, Canese MG, Arico S, Crivelli O, Trepo C, Bonino F, Verme G, Immunofluorescence detection of new antigen-antibody system (delta/anti-delta) associated to hepatitis B virus in liver and in serum of HBsAg carriers. Gut 18, 997–1003 (1977). [PubMed: 75123]
2. Lempp FA, Ni Y, Urban S, Hepatitis delta virus: insights into a peculiar pathogen and novel treatment options. Nature reviews. Gastroenterology & hepatology 13, 580–589 (2016). [PubMed: 27534692]
3. Shirvani-Dastgerdi E, Tacke F, Molecular interactions between hepatitis B virus and delta virus. World J Virol 4, 36–41 (2015). [PubMed: 25964870]
4. Taylor JM, Hepatitis delta virus. Virology 344, 71–76 (2006). [PubMed: 16364738]
5. Winer BY, Ploss A, Determinants of hepatitis B and delta virus host tropism. Curr Opin Virol 13, 109–116 (2015). [PubMed: 26164658]
6. Lutgehetmann M, Mancke LV, Volz T, Helbig M, Allweiss L, Bornscheuer T, Pollok JM, Lohse AW, Petersen J, Urban S, Dandri M, Humanized chimeric uPA mouse model for the study of hepatitis B and D virus interactions and preclinical drug evaluation. Hepatology 55, 685–694 (2012). [PubMed: 22031488]
7. Ponzetto A, Cote PJ, Popper H, Hoyer BH, London WT, Ford EC, Bonino F, Purcell RH, Gerin JL, Transmission of the hepatitis B virus-associated delta agent to the eastern woodchuck. Proc Natl Acad Sci U S A 81, 2208–2212 (1984). [PubMed: 6585793]
8. Taylor J, Mason W, Summers J, Goldberg J, Aldrich C, Coates L, Gerin J, Gowans E, Replication of human hepatitis delta virus in primary cultures of woodchuck hepatocytes. J Virol 61, 2891–2895 (1987). [PubMed: 3612956]
9. Kuo MY, Goldberg J, Coates L, Mason W, Gerin J, Taylor J, Molecular cloning of hepatitis delta virus RNA from an infected woodchuck liver: sequence, structure, and applications. J Virol 62, 1855–1861 (1988). [PubMed: 3367426]
10. Netter HJ, Gerin JL, Tennant BC, Taylor JM, Apparent helper-independent infection of woodchucks by hepatitis delta virus and subsequent rescue with woodchuck hepatitis virus. J Virol 68, 5344–5350 (1994). [PubMed: 8057418]
11. Ni Y, Lempp FA, Mehrle S, Nkongolo S, Kaufman C, Falth M, Stindt J, Koniger C, Nassal M, Kubitz R, Sultmann H, Urban S, Hepatitis B and D viruses exploit sodium taurocholate co-transporting polypeptide for species-specific entry into hepatocytes. Gastroenterology 146, 1070–1083 (2014). [PubMed: 24361467]
12. Yan H, Zhong G, Xu G, He W, Jing Z, Gao Z, Huang Y, Qi Y, Peng B, Wang H, Fu L, Song M, Chen P, Gao W, Ren B, Sun Y, Cai T, Feng X, Sui J, Li W, Sodium taurocholate cotransporting polypeptide is a functional receptor for human hepatitis B and D virus. Elife 1, e00049 (2012). [PubMed: 23150796]
13. Lempp FA, Wiedtke E, Qu B, Roques P, Chemin I, Vondran FW, Le Grand R, Grimm D, Urban S, Sodium taurocholate cotransporting polypeptide is the limiting host factor of Hepatitis B Virus infection in macaque and pig hepatocytes. Hepatology, (2017).
14. Yan H, Peng B, He W, Zhong G, Qi Y, Ren B, Gao Z, Jing Z, Song M, Xu G, Sui J, Li W, Molecular determinants of hepatitis B and D virus entry restriction in mouse sodium taurocholate cotransporting polypeptide. Journal of virology 87, 7977–7991 (2013). [PubMed: 23678176]
15. Li H, Zhuang Q, Wang Y, Zhang T, Zhao J, Zhang Y, Zhang J, Lin Y, Yuan Q, Xia N, Han J, HBV life cycle is restricted in mouse hepatocytes expressing human NTCP. Cell Mol Immunol 11, 175–183 (2014). [PubMed: 24509445]
16. Lempp FA, Qu B, Wang YX, Urban S, Hepatitis B Virus Infection of a Mouse Hepatic Cell Line Reconstituted with Human Sodium Taurocholate Cotransporting Polypeptide. J Virol 90, 4827–4831 (2016). [PubMed: 26865711]
17. He W, Cao Z, Mao F, Ren B, Li Y, Li D, Li H, Peng B, Yan H, Qi Y, Sun Y, Wang F, Sui J, Li W, Modification of Three Amino Acids in Sodium Taurocholate Cotransporting Polypeptide Renders

Mice Susceptible to Infection with Hepatitis D Virus In Vivo. J Virol 90, 8866–8874 (2016). [PubMed: 27466423]

18. He W, Ren B, Mao F, Jing Z, Li Y, Liu Y, Peng B, Yan H, Qi Y, Sun Y, Guo JT, Sui J, Wang F, Li W, Hepatitis D Virus Infection of Mice Expressing Human Sodium Taurocholate Co-transporting Polypeptide. PLoS Pathog 11, e1004840 (2015). [PubMed: 25902143]
19. Lempp FA, Mutz P, Lipps C, Wirth D, Bartenschlager R, Urban S, Evidence that hepatitis B virus replication in mouse cells is limited by the lack of a host cell dependency factor. J Hepatol 64, 556–564 (2016). [PubMed: 26576481]
20. Winer BY, Huang TS, Pludwinski E, Heller B, Wojcik F, Lipkowitz GE, Parekh A, Cho C, Shrirao A, Muir TW, Novik E, Ploss A, Long-term hepatitis B infection in a scalable hepatic co-culture system. Nature communications 8, 125 (2017).
21. Yang PL, Althage A, Chung J, Chisari FV, Hydrodynamic injection of viral DNA: a mouse model of acute hepatitis B virus infection. Proc Natl Acad Sci U S A 99, 13825–13830 (2002). [PubMed: 12374864]
22. Giersch K, Homs M, Volz T, Helbig M, Allweiss L, Lohse AW, Petersen J, Buti M, Pollicino T, Sureau C, Dandri M, Lutgehetmann M, Both interferon alpha and lambda can reduce all intrahepatic HDV infection markers in HBV/HDV infected humanized mice. Sci Rep 7, 3757 (2017). [PubMed: 28623307]
23. Polson AG, Bass BL, Casey JL, RNA editing of hepatitis delta virus antigenome by dsRNA-adenosine deaminase. Nature 380, 454–456 (1996). [PubMed: 8602246]
24. Polson AG, Ley HL, 3rd, Bass BL, Casey JL, Hepatitis delta virus RNA editing is highly specific for the amber/W site and is suppressed by hepatitis delta antigen. Mol Cell Biol 18, 1919–1926 (1998). [PubMed: 9528763]
25. Lee CM, Bih FY, Chao YC, Govindarajan S, Lai MM, Evolution of hepatitis delta virus RNA during chronic infection. Virology 188, 265–273 (1992). [PubMed: 1566577]
26. Deny P, Hepatitis delta virus genetic variability: from genotypes I, II, III to eight major clades? Curr Top Microbiol Immunol 307, 151–171 (2006). [PubMed: 16903225]
27. Casey JL, Tennant BC, Gerin JL, Genetic changes in hepatitis delta virus from acutely and chronically infected woodchucks. J Virol 80, 6469–6477 (2006). [PubMed: 16775334]
28. Petersen J, Dandri M, Mier W, Lutgehetmann M, Volz T, von Weizsacker F, Haberkorn U, Fischer L, Pollok JM, Erbes B, Seitz S, Urban S, Prevention of hepatitis B virus infection in vivo by entry inhibitors derived from the large envelope protein. Nat Biotechnol 26, 335–341 (2008). [PubMed: 18297057]
29. Blank A, Markert C, Hohmann N, Carls A, Mikus G, Lehr T, Alexandrov A, Haag M, Schwab M, Urban S, Haefeli WE, First-in-human application of the novel hepatitis B and hepatitis D virus entry inhibitor myrcludex B. J Hepatol 65, 483–489 (2016). [PubMed: 27132172]
30. Frei AP, Bava FA, Zunder ER, Hsieh EW, Chen SY, Nolan GP, Gherardini PF, Highly multiplexed simultaneous detection of RNAs and proteins in single cells. Nat Methods 13, 269–275 (2016). [PubMed: 26808670]
31. Gripon P, Cannie I, Urban S, Efficient inhibition of hepatitis B virus infection by acylated peptides derived from the large viral surface protein. J Virol 79, 1613–1622 (2005). [PubMed: 15650187]
32. Bogomolov P, Alexandrov A, Voronkova N, Macievich M, Kokina K, Petrachenkova M, Lehr T, Lempp FA, Wedemeyer H, Haag M, Schwab M, Haefeli WE, Blank A, Urban S, Treatment of chronic hepatitis D with the entry inhibitor myrcludex B: First results of a phase Ib/IIa study. Journal of hepatology 65, 490–498 (2016). [PubMed: 27132170]
33. Bordier BB, Marion PL, Ohashi K, Kay MA, Greenberg HB, Casey JL, Glenn JS, A prenylation inhibitor prevents production of infectious hepatitis delta virus particles. J Virol 76, 10465–10472 (2002). [PubMed: 12239323]
34. Koh C, Canini L, Dahari H, Zhao X, Uprichard SL, Haynes-Williams V, Winters MA, Subramanya G, Cooper SL, Pinto P, Wolff EF, Bishop R, Ai Thanda Han M, Cotler SJ, Kleiner DE, Keskin O, Idilman R, Yurdaydin C, Glenn JS, Heller T, Oral prenylation inhibition with lonafarnib in chronic hepatitis D infection: a proof-of-concept randomised, double-blind, placebo-controlled phase 2A trial. Lancet Infect Dis 15, 1167–1174 (2015). [PubMed: 26189433]

35. Guidotti LG, Matzke B, Schaller H, Chisari FV, High-level hepatitis B virus replication in transgenic mice. J Virol 69, 6158–6169 (1995). [PubMed: 7666518]

36. Giersch K, Allweiss L, Volz T, Helbig M, Bierwolf J, Lohse AW, Pollok JM, Petersen J, Dandri M, Lutgehetmann M, Hepatitis Delta co-infection in humanized mice leads to pronounced induction of innate immune responses in comparison to HBV mono-infection. J Hepatol 63, 346–353 (2015). [PubMed: 25795587]

37. Suarez-Amaran L, Usai C, Di Scala M, Godoy C, Ni Y, Hommel M, Palomo L, Segura V, Olague C, Vales A, Ruiz-Ripa A, Buti M, Salido E, Prieto J, Urban S, Rodriguez-Frias F, Aldabe R, Gonzalez-Aseguinolaza G, A new HDV mouse model identifies mitochondrial antiviral signaling protein (MAVS) as a key player in IFN-beta induction. J Hepatol, (2017).

38. Protzer U, Maini MK, Knolle PA, Living in the liver: hepatic infections. Nat Rev Immunol 12, 201–213 (2012). [PubMed: 22362353]

39. Sells MA, Chen ML, Acs G, Production of hepatitis B virus particles in Hep G2 cells transfected with cloned hepatitis B virus DNA. Proc Natl Acad Sci U S A 84, 1005–1009 (1987). [PubMed: 3029758]

40. Kuo MY, Chao M, Taylor J, Initiation of replication of the human hepatitis delta virus genome from cloned DNA: role of delta antigen. J Virol 63, 1945–1950 (1989). [PubMed: 2649689]

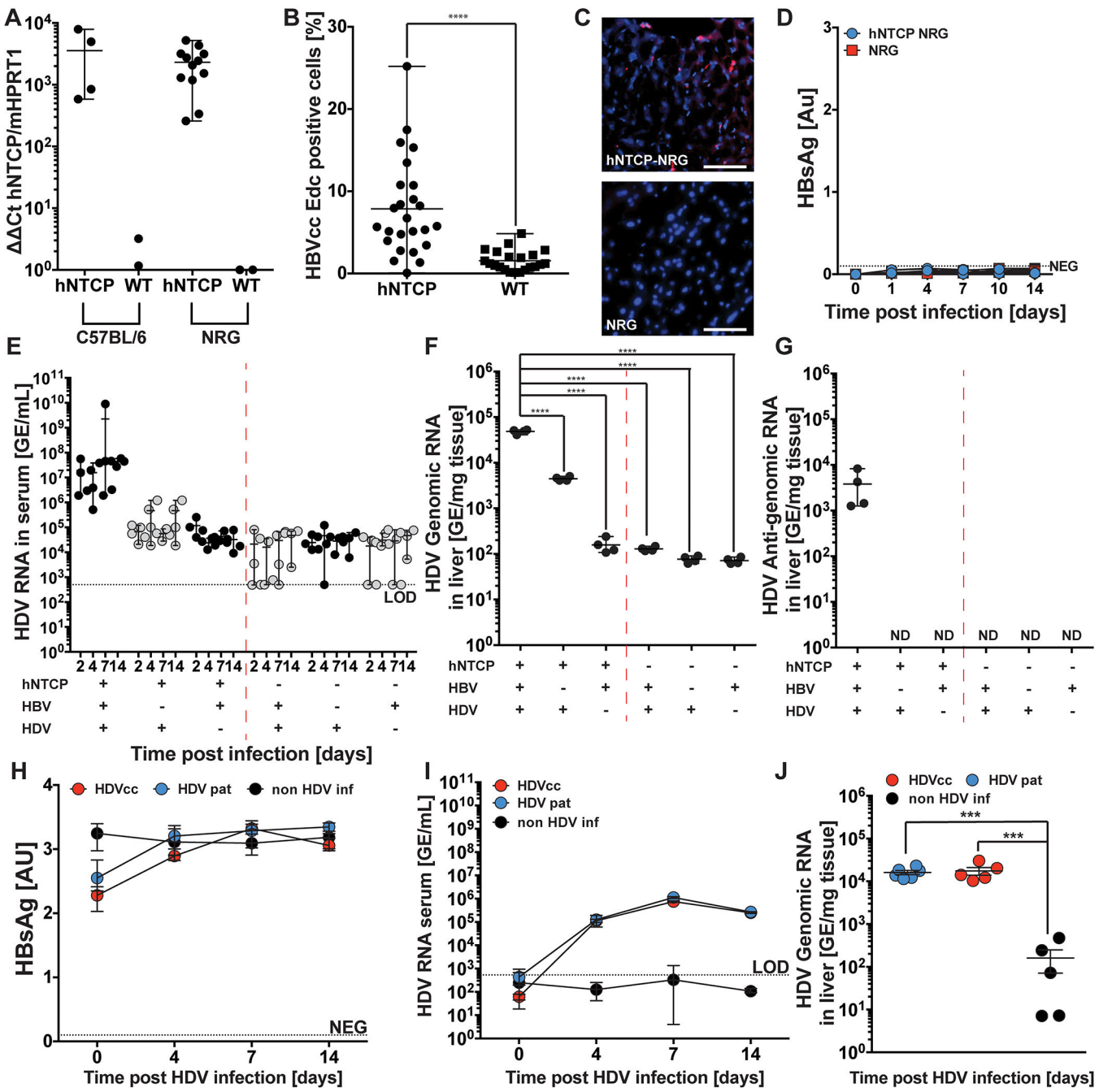

Figure 1. hNTCP-BAC NRG mice facilitate uptake of HBVcc and HDVcc.

(**A**) hNTCP expression levels as compared to housekeeping gene *HPRT1* in hNTCP-BAC C57BL/6 (n=4), hNTCP-NRG (n=12) with C57BL/6 (n=2) and NRG (n=2) mice using relative RT-qPCR and comparing ΔΔCt. Mice were challenged with infectious 5-ethynyl-2′-deoxycytidine (EdC) labeled HBVcc. (**B**) Quantification of HBVcc-EdC entry into murine hepatocytes [percent cells positive for HBV DNA in an entire slide section] of hNTCP-BAC NRG (n=3) versus NRG (n=3) WT animals. (**C**) Representative images of HBVcc-EdC entry in hNTCP-BAC (top) and NRG WT (bottom) hepatocytes. HBV DNA (red) and nuclei

(blue) were observed (scale bar = 200 μm). (**D**) HBsAg quantification over two weeks for hNTCP-BAC NRG (blue, n=5) and NRG WT (red, n=5) mice challenged with HBVcc. Quantitation of HDV RNA in serum (**E**), HDV genomic RNA in liver (**F**), HDV anti-genomic in liver (**G**), in hNTCP-BAC NRG (n=4) versus WT NRG (n=4) mice with or without expression of HBV envelope proteins. The red dashed lines separate the hNTCP-expressing (left) from non-expressing mice (right) in each of the panels. hNTCP-BAC/1.3× HBV HDD NRG mice were challenged with patient-derived HDV virions (HDVpat n=6), HDVcc, or were non-infected. (**H**) Longitudinal HBsAg data, (**I**). Longitudinal HDV RNA in the serum of animals and (**J**). Quantification of genomic HDV RNA in the liver. All data are represented as ± s.e.m. Statistical significance was as follows: *, $p < 0.05$; **, $p \leq 0.001$, ***, $p \leq 0.001$, ****, $p \leq 0.0001$, using an ordinary one-way ANOVA with a Bonferroni's multiple comparisons test.

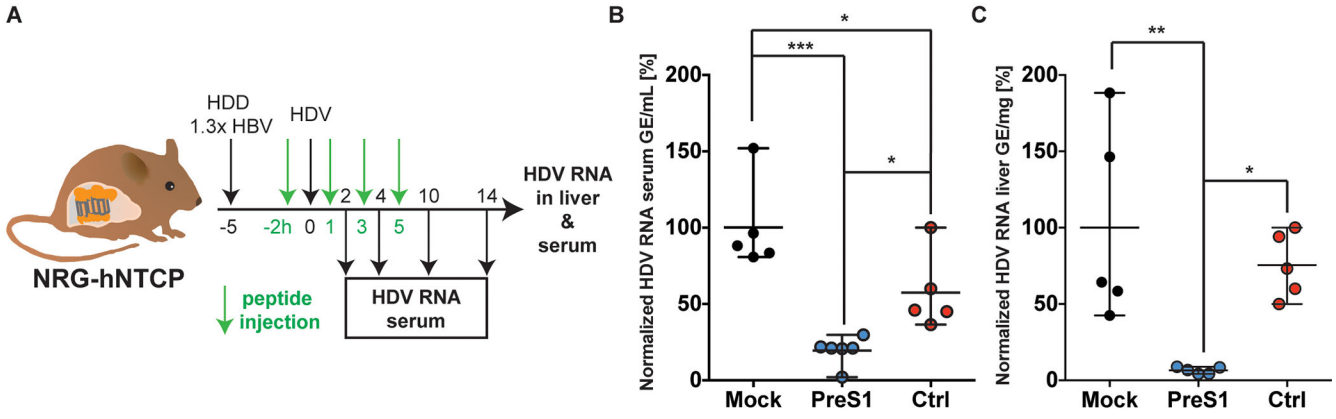

Figure 2. HDV infects hNTCP-BAC/1.3× HBV HDD NRG mice through native entry mechanisms.

(**A**) Schematic of time course for peptide inhibition assay. Normalized quantification of HDV RNA in hNTCP-BAC/1.3×HBV HDD NRG mice treated with mock (black, n=5), preS1-FITC peptide (blue, n=5), or a non-inhibitory control peptide (red, n=5) in serum (**B**) or liver (**C**). All data are represented as ± s.e.m. Statistical significance was as follows: *, $p < 0.05$; **, $p \leq 0.001$, ***, $p \leq 0.001$, ****, $p \leq 0.0001$, using an ordinary one-way ANOVA with a Bonferroni's multiple comparisons test.

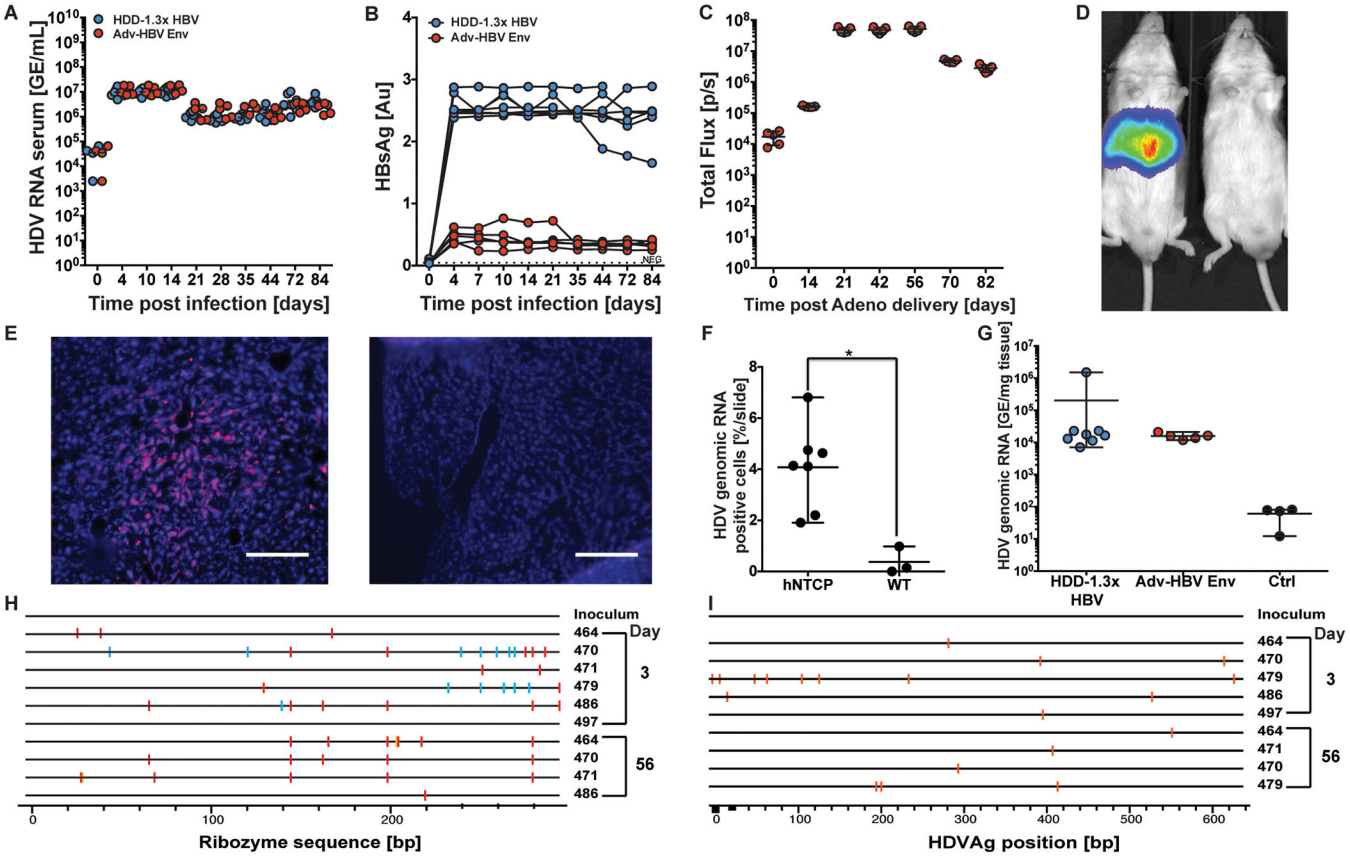

Figure 3. Characterization of persistent HDV infection in hNTCP-BAC NRG mice.

hNTCP-BAC/1.3× HBV HDD NRG (blue, n=8) or hNTCP-BAC/Adv-HBV Env (red, n=5) mice challenged with HDV. HDV RNA in serum (**A**); HBsAg quantification (**B**); firefly luciferase quantification in mice over time (**C**). (**D**) IVIS image of hNTCP-BAC/AdV HBV Env mouse (left) compared to NRG WT mice (right). (**E**) HDV genomic RNA (red) and DAPI (blue) visualization by PLAYR technique in HDV-challenged hNTCP-BAC/Adv-HBV Env (left) versus NRG WT (right). Scale bar = 200 nM. (**F**) Quantification of HDV genomic RNA in hNTCP-BAC/Adv-HBV Env versus NRG WT mice [percent cells HDV RNA positive/slide imaged]. (**G**) HDV RNA quantification by RT-qPCR in the liver of hNTCP-BAC/1.3× HBV (blue), hNTCP-BAC/Adv-HBV env (red), and NRG WT mice (black). (**H**) Highlighter plot of ribozyme domain in hNTCP-BAC/1.3× HBV HDD mice at day 3 and day 56 p.i. (red = transversion mutations, light blue = transition mutations). (**I**) Highlighter plot of HDVAg sequence for hNTCP-BAC/1.3× HBV NRG animals (orange = non-synonymous mutations). All data are represented as ± s.e.m. Statistical significance was as follows: *, $p < 0.05$; **, $p \leq 0.001$, ***, $p \leq 0.001$, ****, $p \leq 0.0001$, using an ordinary one-way ANOVA with a Bonferroni's multiple comparisons test.

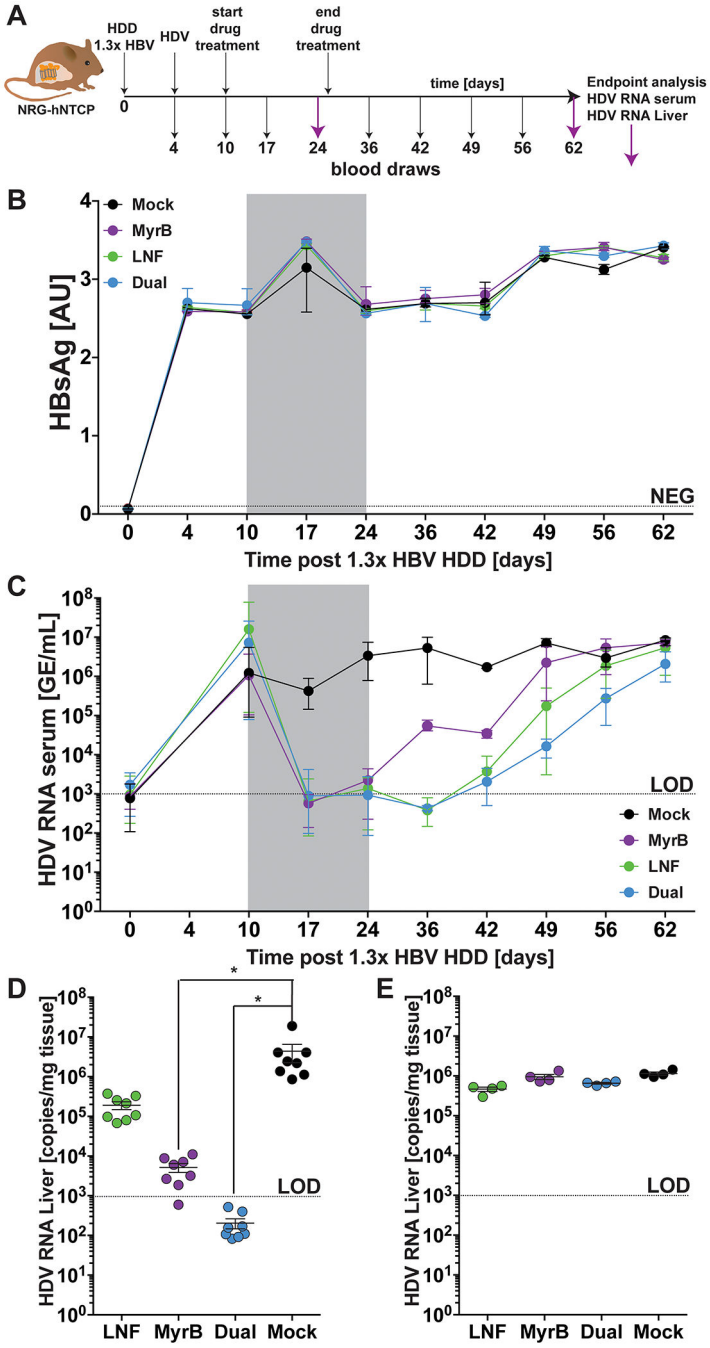

Figure 4. Single and combination therapy with Myrcludex B and Lonafarnib efficiently suppresses HDV viremia *in vivo*.

(**A**) Schematic of drug treatment experimental time course. (**B**) Longitudinal HBsAg ELISA data. (**C**) Longitudinal analysis of HDV RNA in serum of mock carrier control, LNF, MyrB, and dually treated groups. (**D**) HDV RNA in liver at the treatment endpoint (18 days post HDV infection, 14 days post drug treatment) (n=6 for each treatment condition). (**E**) HDV RNA in liver of HDV-challenged hNTCP-BAC NRG mice that had drug treatment stopped (n=4 for each drug condition). All data are represented as ± s.e.m. Statistical significance

was as follows: *, $p < 0.05$; **, $p \leq 0.001$, ***, $p \leq 0.001$, ****, $p \leq 0.0001$, using an ordinary one-way ANOVA with a Bonferroni's multiple comparisons test.

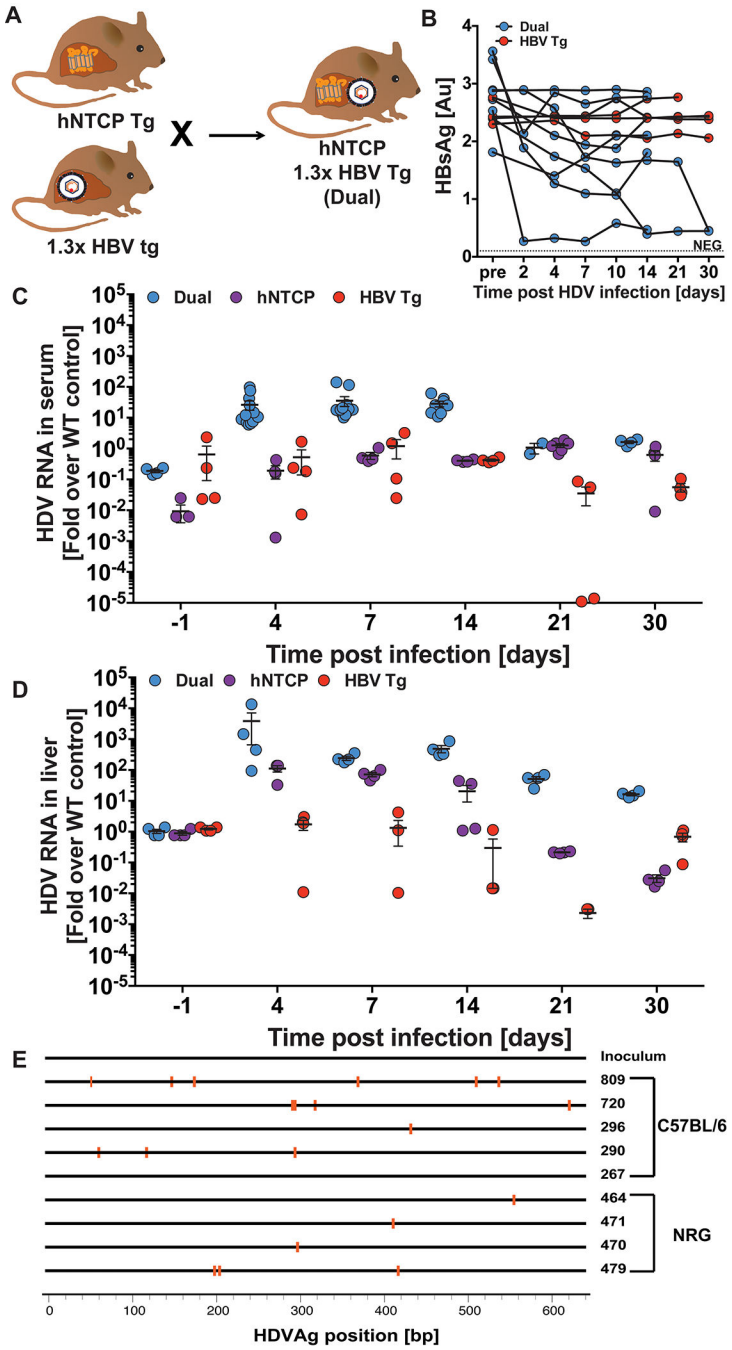

Figure 5. Characterization of HDV acute infection in immunocompetent hNTCP-BAC C57BL/6 mice.

(**A**) Schematic of hNTCP-BAC C57BL/6 and 1.3× HBV tg mice crossed to generate hNTCP-BAC/1.3× HBV Tg C57BL/6 mice. (**B**) HBsAg quantification of hNTCP-BAC/1.3× HBV tg versus HBV tg mice over a month's time. NEG = indicates the threshold for the assay above which HBsAg levels are considered positive. Normalized HDV RNA in serum (**C**) and liver (**D**) of hNTCP-BAC/1.3× HBV tg, hNTCP-BAC tg, and HBV tg animals. (**E**) Highlighter plot analysis of HDVAg sequences in immunocompetent hNTCP-BAC/1.3×

HBV tg C57BL/6 mice (day 14) versus hNTCP-BAC/1.3× HBV NRG mice (day 56) (red= site of mutation). For each time point, hNTCP only (n=4), hNTCP-BAC/1.3× HBV tg (n=4), and HBV tg (n=4) mice were euthanized. All data are represented as ± s.e.m. Statistical significance was as follows: *, $p < 0.05$; **, $p \leq 0.001$, ***, $p \leq 0.001$, ****, $p \leq 0.0001$, using an ordinary one-way ANOVA with a Bonferroni's multiple comparisons test.

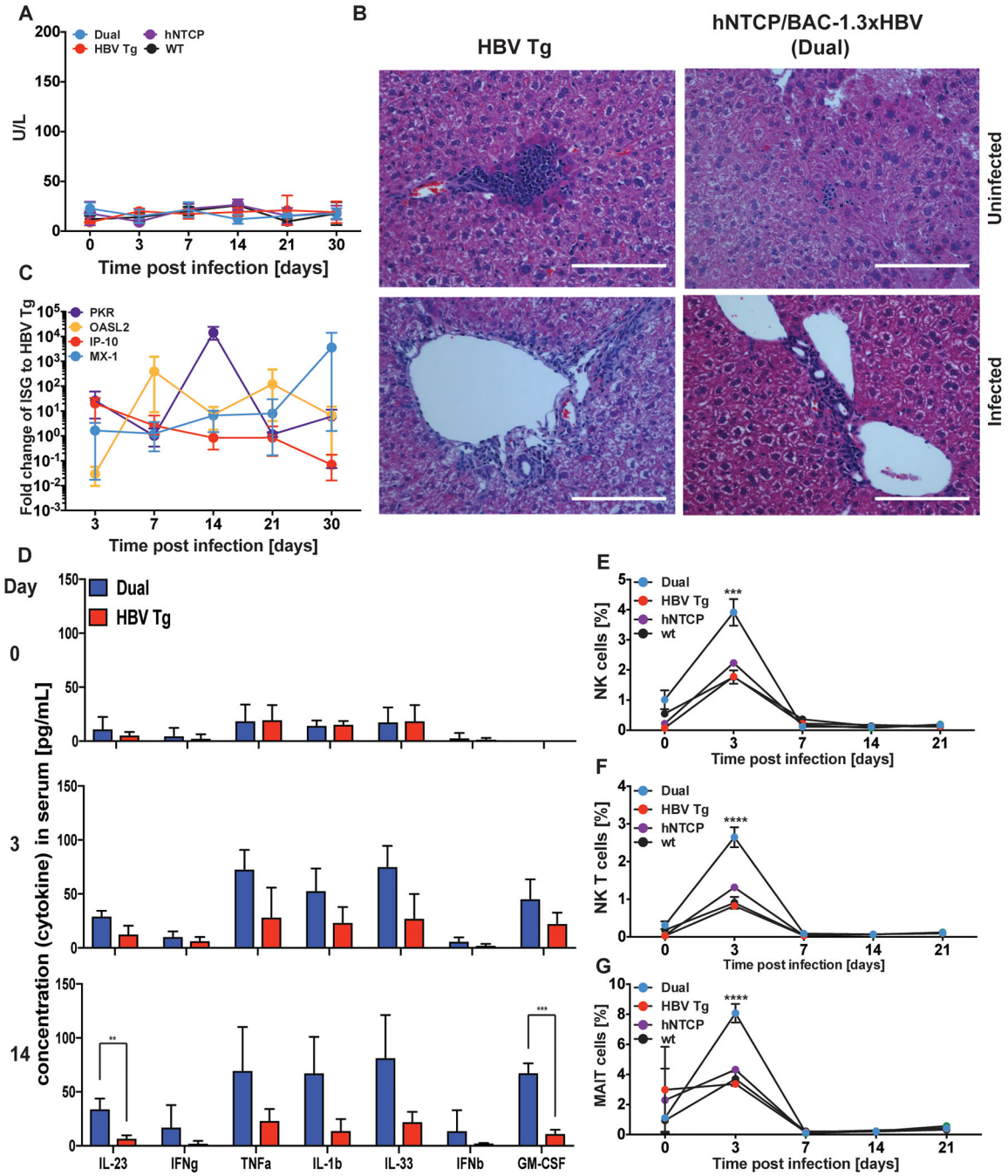

Figure 6. Characterization of histopathology in HDV challenged hNTCP-BAC/1.3× HBV Tg animals.

(**A**) ALT levels for hNTCP-BAC/1.3× HBV tg, hNTCP-BAC tg, HBV tg, and WT animals. (**B**) Histopathological analysis of the liver from hNTCP-BAC/1.3× HBV tg and HBV tg animals. Scale bar = 400 μm. (**C**) Normalized fold change of ISGs MX1, IP-10, OASL2, and PKR in the livers of hNTCP-BAC/1.3× HBV tg animals compared to HBV tg. (**D**) Cytokine analysis in sera of HDV-challenged hNTCP-BAC/1.3× HBV and HBV tg C57BL/6 animals at days 0, 3, and 14 p.i. Cellular immune response in the spleens of HDV-challenged

hNTCP-BAC/1.3× HBV tg, hNTCP Tg, HBV tg, and WT mice: NK cells (**E**); NKT cells (**F**); and MAIT cells (**G**). Frequencies of CD45+ lymphocytes are indicated. Each data point is the average of four different animals. All data are represented as ± s.e.m. Statistical significance was as follows: *, $p < 0.05$; **, $p \leq 0.001$, ***, $p \leq 0.001$, ****, $p \leq 0.0001$, using an ordinary one-way ANOVA with a Bonferroni's multiple comparisons test.